J. Fluid Mech. (1989), *vol.* 203, *pp.* 517–524
Printed in Great Britain

Inertial migration of a sphere in Poiseuille flow

By JEFFREY A. SCHONBERG AND E. J. HINCH
Department of Applied Mathematics and Theoretical Physics, University of Cambridge, Silver Street, Cambridge CB3 9EW, UK

(Received 3 October 1988)

The inertial migration of a small sphere in a Poiseuille flow is calculated for the case when the channel Reynolds number is of order unity. The equilibrium position is found to move towards the wall as the Reynolds number increases. The migration velocity is found to increase more slowly than quadratically. These results are compared with the experiments of Segré & Silberberg (1962*a*, *b*).

1. Introduction

The inertial migration of neutrally buoyant spheres was first documented experimentally by Segré & Silberberg (1962*a*, *b*) and has since been investigated theoretically by Cox & Brenner (1968), Vasseur & Cox (1976), and Ho & Leal (1974). A dilute suspension of neutrally buoyant spheres caused to flow in a pipe develops concentration gradients. As the suspension flows under laminar conditions, the concentration of spheres decreases near the centreline of the pipe, and shows an even larger decrease near the wall. Meanwhile the concentration of the spheres increases at intermediate radial positions, as the spheres tend to collect at an equilibrium radial position 0.6 of a pipe radius from the centreline. This effect may explain why the apparent viscosity of a dilute suspension appears under some flow conditions to be lower than that predicted by Einstein's result (Segré & Silberberg 1962*b*). Ho & Leal provide a good review of this phenomenon.

The migration is due to the inertia of the fluid and the successful theories have included wall effects as well as the convective acceleration. This has been achieved through a *regular* perturbation of the creeping flow equations, and leads to a correct prediction of the equilibrium radial position (Ho & Leal 1974: Vasseur & Cox 1976 implementing the solution method of Cox & Brenner 1968). For these theories to be valid, the channel Reynolds number R_c must be small:

$$R_c = U_m l/\nu \leqslant 1,$$

where U_m is the maximum velocity and l the channel width. This restriction avoids the Whitehead paradox and the necessity of an Oseen analysis, because the presence of the walls limits the lengthscales and so ensures that the local Reynolds number is small everywhere. The data, on the other hand, were collected by Segré & Silberberg (1962*b*) under conditions of higher pipe Reynolds number, from 2 to 700. Furthermore, for pipe Reynolds numbers greater than 30, the radial equilibrium position was found to move closer to the wall and the migration velocity increase more slowly than quadratically with the mean velocity; and these effects are not explained by the current theories.

The present theory employs a *singular* perturbation expansion with an Oseen-like region in which the convective terms are comparable to the viscous terms. By assuming that the sphere is sufficiently small, the disturbance of the background flow will be small so that the convective terms can be linearized. The work is thus based on the framework of Saffman (1965) except that in this study the background flow is the full parabolic Poiseuille flow. Finally, wall effects are included through the parallel plate geometry and resultant boundary conditions on the Oseen region.

2. Governing equations

The flow configuration is illustrated in figure 1. The Poiseuille flow occurs between two infinite parallel plates and is disturbed by a sphere. The origin of the coordinate system is taken to be instantaneously at the centre of the sphere, and translating relative to the walls with the Poiseuille flow velocity evaluated at the origin. If the sphere were simply swept along by the undisturbed flow then its centre would remain at the origin. The difference between the actual flow and the Poiseulle flow will be called the disturbance flow and is governed by

$$\mu\nabla^2\boldsymbol{u}-\nabla p = \rho\left[\frac{\partial \boldsymbol{u}}{\partial t}+\bar{\boldsymbol{u}}\cdot\nabla\boldsymbol{u}+\boldsymbol{u}\cdot\nabla\bar{\boldsymbol{u}}+\boldsymbol{u}\cdot\nabla\boldsymbol{u}+\boldsymbol{U}_{\mathrm{p}}\cdot\nabla\bar{\boldsymbol{u}}\right],$$

$$\nabla\cdot\boldsymbol{u}=0,$$

$$\boldsymbol{u}=\boldsymbol{U}_{\mathrm{p}}+\boldsymbol{\Omega}_{\mathrm{p}}\wedge\boldsymbol{r}-\bar{\boldsymbol{u}}(z)\quad\text{on}\quad r=a,$$

$$\boldsymbol{u}=0\quad\text{on}\quad z=-d\quad\text{and on}\quad z=l-d,$$

$$\boldsymbol{u}\sim 0\quad\text{as}\quad x\rightarrow\infty,$$

where $\bar{\boldsymbol{u}}$ is the undisturbed Poiseuille flow, $\boldsymbol{U}_{\mathrm{p}}$ and $\boldsymbol{\Omega}_{\mathrm{p}}$ are the translation and rotational velocities of the sphere, and d is the lateral distance of the sphere from the wall as shown in figure 1. (We are indebted to Dr H. A. Stone for correcting our omission of the last term in the momentum equation, which arises from the acceleration of our chosen coordinate frame.)

Let the ratio of the small radius of the sphere a compared with the channel width l be denoted by

$$\alpha = a/l.$$

In the moving reference frame the Poiseuille flow is then

$$\bar{\boldsymbol{u}} = U_{\mathrm{m}}[\alpha\gamma z/a-4\alpha^2z^2/a^2,0,0],$$

where U_{m} is the maximum velocity of the Poiseuille flow and γ is the shear rate non-dimensionalized by U_{m} and l, and is given by

$$\gamma = 4-8d/l.$$

A particle Reynolds number can then be defined in terms of the size of the sphere and the shear rate by

$$R_{\mathrm{p}} = U_{\mathrm{m}}a^2/\nu l = \alpha^2 R_{\mathrm{c}}.$$

Both the particle Reynolds number R_{p} and the relative radius of the sphere α are small in much of the data of Silgré & Silberberg (1962*b*). The channel Reynolds number R_{c} is however of order unity or larger. Thus an analysis based on matched asymptotic expansions is suggested.

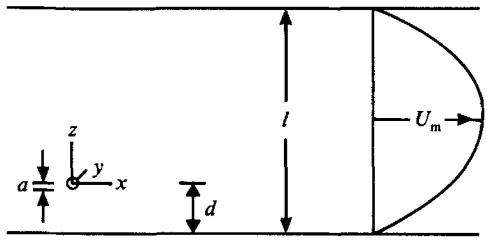

FIGURE 1. Characteristic lengths and velocity; coordinate system and lateral position.

3. The inner problem

In the inner problem we focus on the sphere, scaling the Navier–Stokes equations by the sphere radius a and the Poiseuille velocity (relative to the walls) at the centreplane U_m. In the limit of R_p and α small the governing equation reduces to a creeping flow problem in an infinite fluid driven by the $O(\alpha)$ shear on the sphere. An expansion may thus be posed:

$$\boldsymbol{u} \sim \alpha \boldsymbol{u}_0,$$

where $\boldsymbol{u}_0$ satisfies

$$\nabla^2 \boldsymbol{u}_0 - \nabla p_0 = 0,$$

$$\nabla \cdot \boldsymbol{u}_0 = 0,$$

$$\boldsymbol{u}_0 = \boldsymbol{U}_{p0} + \boldsymbol{\Omega}_{p0} \wedge \boldsymbol{r} - \gamma z \boldsymbol{e}_1 \quad \text{on} \quad r = 1,$$

$$\boldsymbol{u}_0 \sim 0 \quad \text{as} \quad \boldsymbol{r} \rightarrow \infty.$$

The translational and rotational velocities of the sphere are determined by the condition that there is no net force and torque for the neutrally buoyant spheres which does not accelerate at this order. Batchelor (1967) finds

$$\boldsymbol{u}_0 = -5\gamma xz\boldsymbol{r}/2r^5 + O(r^{-4}) \quad \text{as} \quad r \rightarrow \infty$$

and

$$\boldsymbol{U}_{p0} = 0.$$

Thus there is no lateral migration at this order.

An $O(\alpha^2)$-correction to the above $O(\alpha)$-solution arises from the curvature of the Poiseuille flow. This velocity decays more rapidly, like r^{-3} (Schonberg, Drew & Belfort 1986). Owing to the reversibility of Stokes flow this correction also gives rise to no lateral motion. The regular perturbation correction from inertia in the inner region is of order $R_p \alpha$ and this also gives no migration from the symmetry (Cox & Brenner 1968).

4. The outer problem

Now while the leading-order viscous solution is fairly short range, decaying like $O(r^{-2})$, it does not decay exponentially and so an Oseen expansion must be considered in which viscous terms balance acceleration terms. In this outer region a new coordinate $\boldsymbol{R}$ is introduced which is the inner coordinate $\boldsymbol{r}$ stretched by some power of the particle Reynolds number. The motion in this region is driven by the longest range portion of the leading-order viscous field. With the scaling

$$\boldsymbol{R} = R_p^{\frac{1}{2}} \boldsymbol{r}$$

the velocity expansion required is

$$\boldsymbol{u} \sim \alpha R_{\mathrm{p}} \boldsymbol{U}_0$$

satisfying

$$\nabla^2 \boldsymbol{U}_0 - \nabla P_0 = (\gamma Z - 4R_{\mathrm{c}}^{-\frac{1}{2}} Z^2)\frac{\partial \boldsymbol{U}_0}{\partial X} + W_0 \boldsymbol{e}_1(\gamma - 8R_{\mathrm{c}}^{-\frac{1}{2}} Z),$$

$$\nabla \cdot \boldsymbol{U}_0 = 0,$$

$$\boldsymbol{U}_0 \sim -5\gamma XZ\boldsymbol{R}/2R^5 \quad \text{as} \quad \boldsymbol{R} \to 0,$$

$$\boldsymbol{U}_0 = 0 \quad \text{on} \quad Z = -R_{\mathrm{c}}^{\frac{1}{2}} d/l \quad \text{and on} \quad Z = R_{\mathrm{c}}^{\frac{1}{2}}(l-d)/l.$$

Note that at this order of aproximation the convective terms are linearized, so that the velocity disturbance in the wake does not interact with itself. Also the time-derivative term is negligible because the migration velocity is small.

Now if the regular part of $\boldsymbol{U}_0$ is non-zero at the origin, there will be a corresponding uniform flow in the inner region of order αR_{p}. As the sphere is force-free, it must follow this uniform flow. Thus there will be a lateral migration velocity

$$W_{\mathrm{p}} = \alpha R_{\mathrm{p}} \lim_{\boldsymbol{R}\to 0} \{W_0(\boldsymbol{R}) + 5\gamma XZ^2/2R^5\}.$$

There are further correction terms in the outer expansion. Two of order $\alpha^2 R_{\mathrm{p}}^{\frac{3}{2}}$ and αR_{p}^2 match the next parts of the leading-order inner solution of order $\alpha^2 r^{-3}$ and αr^{-4} respectively. There are also regular corrections of the outer solution of order $\alpha R_{\mathrm{p}}^{\frac{5}{2}}$ and $\alpha^2 R_{\mathrm{p}}^2$. Hence if $\alpha \ll 1$ and $R_{\mathrm{p}} \ll 1$, the estimate of the migration velocity given above is the leading-order term. This singular perturbation approach was presented for the special case of R_{c} large by Schonberg (1986).

The next phase of the development is to recast the outer problem for $\boldsymbol{U}_0$. Following Saffman (1965), the matching condition as $\boldsymbol{R} \to 0$ is equivalent to a singularity in the governing momentum equation corresponding to the symmetric force dipole (Schonberg *et al.* 1989):

$$-10\pi\gamma/3\left[\frac{\partial}{\partial Z}, 0, \frac{\partial}{\partial X}\right]\delta(\boldsymbol{R}).$$

The governing equations may then be Fourier transformed in the plane parallel to the walls:

$$\tilde{\boldsymbol{U}}_0(k_1, k_2, Z) = \frac{1}{4\pi^2}\int_{-\infty}^{\infty}\int_{-\infty}^{\infty} \boldsymbol{U}_0(X, Y, Z)\, \mathrm{e}^{-\mathrm{i}(k_1 X + k_2 Y)}\, \mathrm{d}X\, \mathrm{d}Y,$$

to yield coupled ordinary differential equations in the cross-stream structure. It is then possible to eliminate in favour of the lateral component of the transformed velocity $\tilde{W}_0$ and the transformed pressure $\tilde{P}$:

$$\frac{\mathrm{d}^2\tilde{P}}{\mathrm{d}Z^2} - (k_1^2 + k_2^2)\tilde{P} = -2(\gamma - 8R_{\mathrm{c}}^{-\frac{1}{2}} Z)\,\mathrm{i}k_1 \tilde{W}_0,$$

$$\frac{\mathrm{d}^2\tilde{W}_0}{\mathrm{d}Z^2} - (k_1^2 + k_2^2)\tilde{W}_0 = \frac{\mathrm{d}\tilde{P}}{\mathrm{d}Z} + (\gamma Z - 4R_{\mathrm{c}}^{-\frac{1}{2}} Z^2)\,\mathrm{i}k_1 \tilde{W}_0.$$

The forcing by the $\delta(Z)$ and its derivatives can be replaced by jump conditions across $Z = 0$:

$$\tilde{P}(k_1, k_2, 0+) - \tilde{P}(k_1, k_2, 0-) = 5\gamma \mathrm{i}k_1/3\pi$$

and

$$\frac{\mathrm{d}\tilde{W}_0}{\mathrm{d}Z}(k_1, k_2, 0+) - \frac{\mathrm{d}\tilde{W}_0}{\mathrm{d}Z}(k_1, k_2, 0-) = 5\gamma \mathrm{i}k_1/6\pi.$$

A NAG routine was used to solve the finite-difference version of these coupled equations. This method worked well to large values of k, e.g. 40, when channel Reynolds number R_c was small, but the method failed to converge when R_c was large, e.g. 150, especially when the particle was near to the wall.

Finally the lateral migration velocity can be found by by synthesizing the Fourier modes, noting that the singular part is purely imaginary and the lateral velocity is purely real:

$$W_p = \alpha R_p \operatorname{Re}\left\{\int_{-\infty}^{\infty}\int_{-\infty}^{\infty} \tilde{W}_0(k_1\, k_2, 0)\,\mathrm{d}k_1\,\mathrm{d}k_2\right\}.$$

The integration was performed in polar coordinates, using a symmetry to restrict attention to the first quadrant. In order to make the integral to infinity converge quite large values of k were required, and these could cause difficulties with the differential-equation solver. To assist the convergence of the integration the first two terms in a regular asymptotic expansion (the first term is purely imaginary) were found and then a Shank's transform was applied.

5. Results

The migration velocity was computed for four values of the channel Reynolds number: 1, 5, 15 and 75. The profiles are shown in figures 2 and 3. Note that the lateral migration velocity is an odd function of position across the centreline of the channel. The first three profiles are almost identical and are close to the results of Vasseur & Cox (1976), which assumed a small channel Reynolds number R_c. The fourth profile is markedly different, with the scaled migration velocities lower and the equilibrium position closer to the wall. This trend is shown in figure 4, which shows a partial profile for a channel Reynolds number of 150. This reduction in the scaled migration velocities is consistent with theoretical results for large R_c which give a lateral velocity smaller than αR_p unless the sphere is quite close to one of the walls, $d = O(lR_c^{-\frac{1}{2}})$ (Schonberg *et al.* 1989). The change in the equilibrium position is shown in figure 5. The results are incomplete owing to numerical difficulties when the channel Reynolds number was extreme. At $R_c = 150$ the equilibrium position could be extrapolated, but not at $R_c = 225$.

6. Comparison with experiments

Even though the theory is for the geometry of a channel, the results are in good agreement with the data of Segré & Silberberg (1962*b*) for a pipe. They found the equilibrium position in several experiments in which the pipe Reynolds number varied from 3 to 30, the particle radius varied from 0.4 mm to 0.855 mm, and the pipe diameter was 11.2 mm. This corresponds to particle Reynolds numbers in the range from 0.009 to 0.20, and the ratio of the sphere radius to the pipe diameter α in the range 0.036 to 0.076. Thus these two parameters are small, as the theory requires. The small-sphere restriction may be less well satisfied when the particle is close to the walls, say within 0.2 of tube diameter.

For the above experimental conditions. Segré & Silberberg found that the equilibrium radial position was 63% of the pipe radius (although this was reported as 60% in their abstract). This corresponds to the value of d/l equal to 0.185, which is the value found in this paper. If the second figure in the experimental data is significant, then this theory gives the position more accurately than the previous theories which gave a value of $d/l = 0.2$.

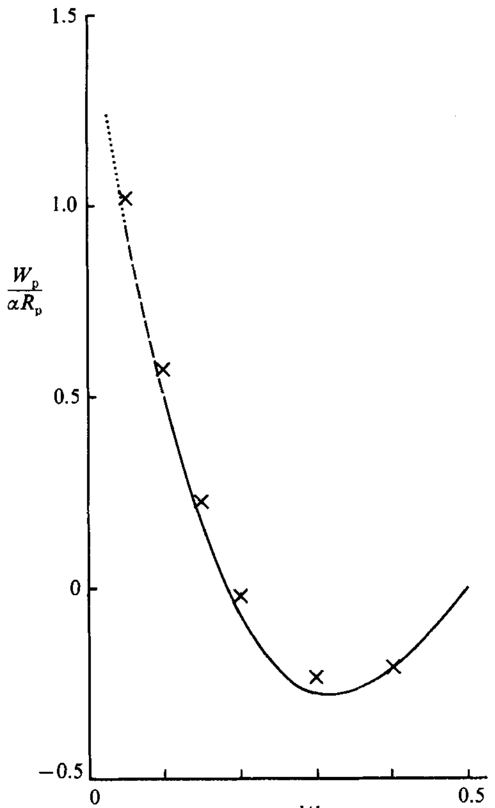

FIGURE 2

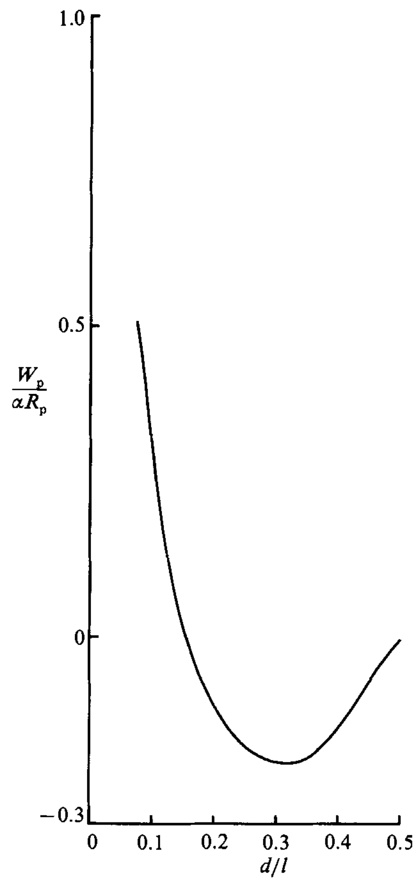

FIGURE 3

FIGURE 2. Lift velocity versus lateral position of the particle: ×, selected points from Vasseur & Cox (1976); ——, $R_c = 1, 5, 15$; ---- $R_c = 5, 15$; ······, $R_c = 15$.

FIGURE 3. Lift velocity versus lateral position of the particle for $R_c = 75$.

At higher pipe Reynolds numbers, Segré & Silberberg noted that the equilibrium position moved towards the wall, as predicted here. This behaviour is reported to have started at a pipe Reynolds number of 30, which is close to the theoretical transition shown in figures 4 and 5. Note that the data are plotted against the channel Reynolds number, which is twice the pipe Reynolds number used by Segré & Silberberg. Experiments at a pipe Reynolds numbers of 43 and 60 gave an equilibrium position of $d/l = 0.16$ and 0.147 respectively in agreement with the theory. It should be noted, however, that in these cases the particle Reynolds number is 0.25 and 0.35 respectively which may not be sufficiently small. Furthermore, the wall was fairly close, within 3 sphere radii. Further experiments were performed at pipe Reynolds numbers of 116 and 172, giving equilibrium positions $d/l = 0.125$ and $d/l = 0.11$. These results agree less well with the theory, although the particle Reynolds number is now 0.68 and 1.00 respectively. Finally some experiments with a pipe Reynolds number of 30 (which were included by Segré & Silberberg in their low-Reynolds-number results) are shown in figure 5 to give $d/l = 0.17$, in good agreement with the theory.

At the higher pipe Reynolds numbers, Segré and Silberberg also noted that the

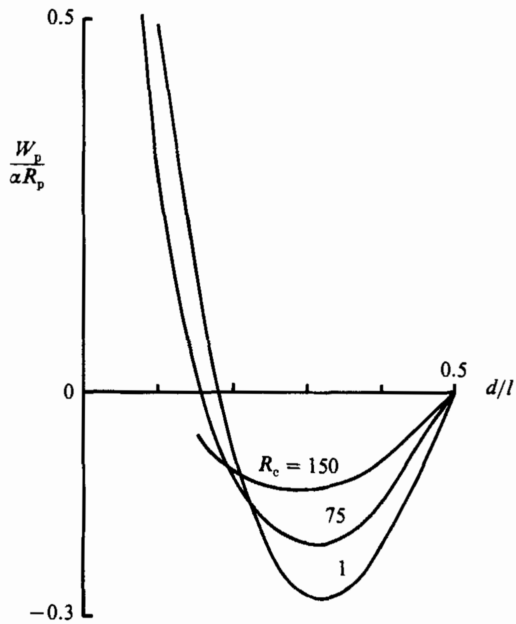

FIGURE 4. Lift velocity versus lateral position of the particle for three channel Reynolds numbers.

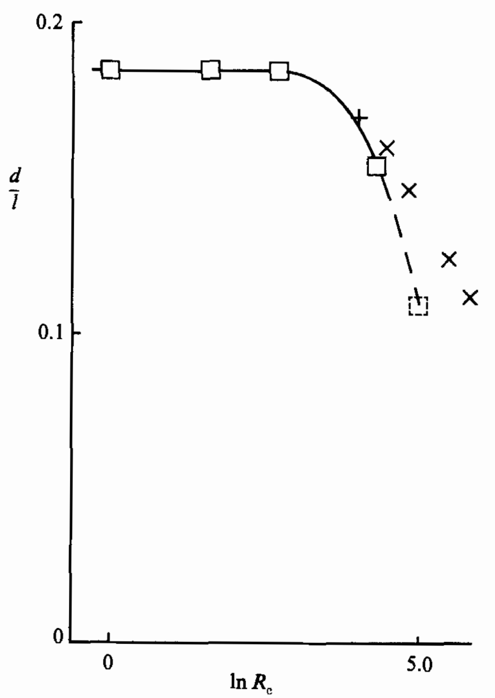

FIGURE 5. Equilibrium position versus channel Reynolds number, theory compared with experiments of Segré & Silberberg (1962*b*): ×, data; +, subset of data (pipe Reynolds number near 30); □, theory; ⬚, extrapolation from partial profile (see figure 4).

dimensionless migration velocities (near the centre of the pipe, where they measured the velocities) were weaker. This is predicted by the theory of this paper.

Ho & Leal (1974) indicated that at their low channel Reynolds numbers the lateral migration was due to the competition of two effects, one linked to the interaction with the wall and the shear there producing a core-ward drift, and one linked to the shear and the curvature of the Poiseuille flow producing a motion towards the wall. Thus there is an equilibrium position midway between the wall and the centre. When the channel Reynolds number exceeds unity, the wake no longer fills the width of the channel as it does at low values. Thus one can expect the inertial interaction with the wall to decrease and be limited to a distance $lR_c^{-\frac{1}{2}}$. This will result in the equilibrium position moving towards the wall to a distance with this scaling. Moreover, within the core, the small width of the wake will reduce the effective measure of the curvature seen by the inertia and so reduce the magnitude of the wall-ward drift there. The small width of the wake and the location of the equilibrium position near the tube wall may explain why the theory developed for a channel seems applicable to the experiments in a pipe.

This work was supported by a NSF NATO Postdoctoral Fellowship held by J.A.S. at the University of Cambridge.

REFERENCES

Batchelor, G. K. 1967 *An Introduction to Fluid Dynamics.* Cambridge University Press.

Cox, R. G. & Brenner, H. 1967 *J. Fluid Mech.* **28**, 391.

Cox, R. G. & Brenner, H. 1968 *Chem. Engng Sci.* **23**, 147.

Ho, B. P. & Leal, L. G. 1974 *J. Fluid Mech.* **65**, 365.

Saffman, P. G. 1965 *J. Fluid Mech.* **22**, 385.

Schonberg, J. A. 1986 Ph.D. thesis, Rensselaer Polytechnic Institute.

Schonberg, J. A., Drew, D. A. & Belfort, G. 1986 *J. Fluid Mech.* **167**, 415.

Segré, G. & Silberberg, A. 1962*a* *J. Fluid Mech.* **14**, 115.

Segré, G. & Silberberg, A. 1962*b* *J. Fluid Mech.* **14**, 136.

Vasseur, P. & Cox, R. G. 1976 *J. Fluid Mech.* **78**, 385.